

## Positive-column plasma studied by fast-flow glow discharge mass spectrometry: Could it be a “Rydberg gas?”

Rod S. Mason,\* Pat D. Miller, Ifor Mortimer, David J. Mitchell, and Neil A. Dash

Department of Chemistry, University of Wales Swansea, Singleton Park, Swansea SA2 8PP, United Kingdom

(Received 14 January 2003; published 23 July 2003)

Ions created from the fast-flowing *positive column* plasma of a glow discharge were monitored using a high voltage magnetic sector mass spectrometer. Since the field gradient and sheath potentials created by the plasma inside the source opposed cation transfer, it is inferred that the ions detected were the field-ionized Rydberg species. This is supported by the mass spectral changes which occurred when a negative bias was applied to the sampling aperture and by the contrasting behavior when attached to a quadrupole analyzer. Reaction with  $H_2$  (titrated into the flowing plasma) quenched not only the ionization of discharge gas Rydberg atoms but also the passage of electric current through the plasma, without significant changes to the field and sheath potentials. Few “free” ions were present and the lifetimes of the Rydberg atoms detected were much longer than seen in lower pressure experiments, indicating additional stabilization in the plasma environment. The observations support the model of the flowing plasma, given previously [R. S. Mason, P. D. Miller, and I. P. Mortimer, Phys. Rev. E 55, 7462 (1997)] as mainly a neutral Rydberg atom gas, rather than a conventional ion-electron plasma.

DOI: 10.1103/PhysRevE.68.016408

PACS number(s): 52.20.-j, 52.80.Hc, 52.25.Ya, 52.50.Dg

### I. INTRODUCTION

The classical definition of the plasma is that it is a partially dissociated gas of high charge density, but overall electrically neutral [1]. It is therefore regarded as containing a high density of “free” ions and electrons, moving randomly, apart from the effect of the electrostatic forces between them. This is widely accepted and is the starting point for most theoretical models. Nevertheless, plasmas are still not completely understood at the molecular level, and their application is often regarded by practitioners as a “black art.”

Direct current glow discharges (GD) have long been an interesting medium for the study of plasmas [1]. In a GD (see Fig. 1), electrons leaving the cathode are accelerated through the *cathode fall* to energies high enough to ionize the discharge gas by electron impact. This happens mainly in the *negative glow* region, where excitation also occurs, together with the emission of light from the excited states formed. At longer distances between the electrodes, the *positive column* links the negative glow region with the anode. The positive column was much studied in the past and is characterized in the older literature by a small positive field in the direction of the anode and a relatively sharp drop in potential from the anode down to the plasma, called the *anode fall* [1,2]. A positive sheath potential at the anode is, however, at odds with the plasma theory, since the plasma ought to be the most positive region of the discharge [1]. An exception can occur if the anode surface area is sufficiently small such that conduction across the boundary forms a rate limiting constriction to the circuit [1,3]. In the older literature [4], the positive column characteristics are made self-consistent with the plasma theory by invoking continuous electron impact ionization within the positive column plasma and at the anode.

This is to replace the ions lost through recombination and radial diffusion and to supply a small positive current towards the cathode. According to this theory, ionization within the plasma is accomplished by electrons in the high-energy tail of the Boltzmann distribution, agitated by the electrical fields generated, particularly across the anode fall. One of the difficulties of this model in relatively high pressure systems is the increased collisional cooling, and short path lengths which make it less likely that electrons formed in the plasma can get accelerated to a high enough energy to ionize a gas such as Ar, at least from the ground state.

Recently, we suggested [5] the heavy involvement of high excited metastable states of neutral Ar to explain the anomalous loss of ionization in the argon-hydrogen plasma. This raises the controversial [6] notion of a truly neutral plasma being created, at least for the plasma conditions of our experiments and similar to those used, for example, in optical emission sources. In further support of this idea we present mass spectrometric evidence for the participation of substantial quantities of neutral Rydberg atoms in the positive column plasma, close to their ionization level, but stabilized by the plasma conditions.

In the classical plasma the electrons move faster than the ions because of the difference in their mass and their higher energies. This leads to a separation of charge at the boundary

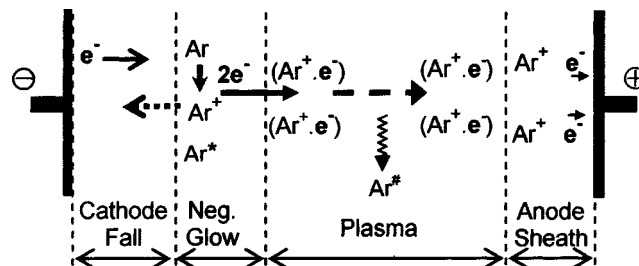


FIG. 1. Schematic showing the different regions of a direct current glow discharge (not to scale—see text) and indicating processes which create the argon plasma.

\*Author to whom correspondence should be addressed; email address: r.s.mason@swan.ac.uk

and a negative sheath potential at the walls containing the plasma, as is commonly observed. The surface at the boundary of such a medium therefore ought to be bombarded by a flux of both cations and electrons. It is indeed possible to detect cations escaping through an aperture in the wall of the contained plasma and mass spectrometry is commonly used as a diagnostic tool [7]. However, success in detecting ions depends on the conditions and the region of the discharge sampled; for example, in the technique of GD mass spectrometry (GDMS) [8,9], used for chemical analysis, analyte ions created in the discharge are sampled through the anode. However, the cations, including those of the discharge gas, are difficult to detect in quantity unless the anode is immersed in the negative glow [9], close to the cathode.

The work described here uses a FFGD ion source, as before [5], in which a discharge is created at one end of the short flow tube and the plasma created flows at high speed onto the sample cone of a double-focusing magnetic deflection mass spectrometer. Low powers ( $<2$  W) were used, creating “cold” flowing plasmas in which it was possible to control the average energy of the plasma species reaching the sampling cone by varying the flow speed of the gas. In these experiments, the field and sheath potentials were monitored, which were consistent with those of a positive column plasma in the flow tube. Copious ions were detected without the aid of an ion extraction voltage, but depending on the flow conditions and the type of the mass spectrometer used [when the fast-flow GD (FFGD) ion source was attached to a quadrupole analyzer relatively few ions were detected [10] for similar conditions, unless a negative bias was applied to the sample cone]. It is inferred that, without a cone bias, detected ions derived from excited neutrals, field ionized outside the cell in the intense ion-beam accelerating field of the double-focusing instrument. With a sufficient cone bias, field ionization of plasma species also occurs inside the cell. This has a peculiar effect in the high voltage instrument such that ion signals, generated by a plasma containing relatively high-energy species, actually decrease with increasing negative bias on the cone.

Gases titrated into the flow allow reactions with these excited state species to be studied directly without interfering with the high electron impact energy region of the cathode fall or the negative glow boundary of the discharge. Reaction with  $H_2$  in a fast-flowing Cu/Ar plasma caused most ions to disappear from the mass spectrum, except for Cu cathode cations which increased significantly. The model presented previously [5] suggested that the ions of the mass spectrum are the products of ionization at the boundary of the plasma from highly excited neutral species. The  $H_2$  effect is caused by quenching reactions of the  $H_2$  with those excited states which are the precursors to the ions detected. The same reaction creates higher concentrations of lower-energy species, e.g., Ar ( $4s, ^3P$ ), which are more reactive with Cu. The experiments described here affirm the previous results, except that the plasma is shown to be much more sensitive to  $H_2$  than indicated previously. Of additional significance, and in further support of the excited state model, the electric current carried by the flowing plasma is also shown to be quenched, but without significant changes to the plasma and sheath po-

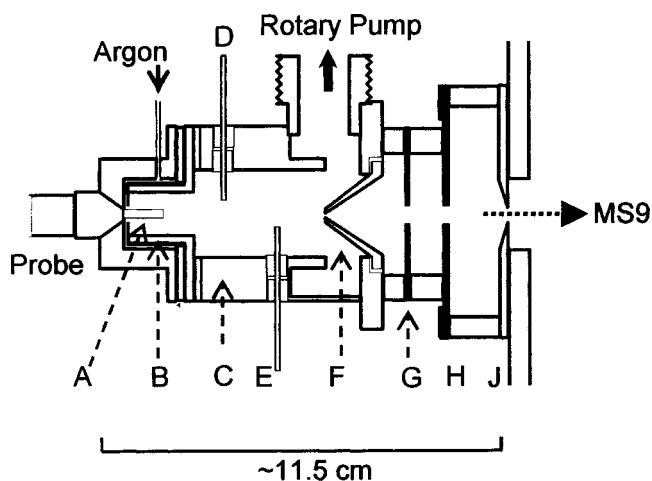


FIG. 2. Cross section through the fast-flow glow discharge ion source: A, cathode (Cu pin); B, anode; C, short flow tube; D and E, combined electrical probes and gas inlets (1 mm od); F, plasma sampling cone, with 0.3-mm-diameter aperture; G, ion-beam focusing and centering plates; H, earth plate; J, adjustable slit at first focal point of the double-focusing (modified MS9) mass spectrometer; and hashed sections are electrically insulating.

tentials. Such behavior is inconsistent with a free ion and electron plasma mechanism and is also at odds with explanations of the anomalous loss of ionization caused by  $H_2$ , as explained based on the free-ion or electron model [11,12]. The involvement of negative ion chemistry is also shown to be negligible.

Only Rydberg species would have sufficient energy to be easily field ionized; they are also highly conducting by charge transfer [13]. It therefore appears that much of the plasma, by the time it reaches the end of the short flow tube, has relaxed into a high concentration of Rydberg species. It is known that such atoms are stabilized by “ $l$  and  $m$ ” mixing [13] in collisions with low-energy electrons and atoms or by electrical fields. Such species, although well studied in low pressure systems, have not been studied previously in a “high” pressure plasma environment. The average lifetimes of the argon Rydberg atoms ( $Ar^R$ ) measured under these conditions are significantly longer than those reported for lower pressure systems; the plasma environment therefore appears to confer additional stabilization. An implication is that Rydberg atom participation could be a significant factor in sustaining the plasma in higher pressure electrical discharges.

## II. APPARATUS AND METHOD

### A. The FFGD source

Brief descriptions of the source were given previously [5,14]. A cross-sectional schematic diagram is shown in Fig. 2. It was designed to fit into the modified source housing of an existing double-focusing magnetic deflection mass spectrometer. The main discharge region was a cylinder B (15×10 mm id), which served as the anode. It was attached to a short flow tube (40×20 mm id). The ion exit was in the form of a cone (given as F) with a 0.3 mm orifice in the

center, the distance through it being 0.25 mm. The cone protruded into the flow by 7.5 mm. The total distance between the end of the copper cathode pin A and the ion exit was 40 mm. The pin measured 2.4 mm in diameter, with a 6 mm length exposed to the discharge. The pin was mounted on the end of a sliding probe, insulated at the end from the probe shaft, and with a removable insulated cap separating the cathode from the anode. The anode, flow tube, and cone were electrically insulated from each other, unless connected by external electrical circuitry. A secondary gas could be titrated through the inlet E (1 mm od), which protruded 7 mm into the plasma and was 8 mm from the aperture. It was electrically insulated from the block and also served as one of the three probes (not all shown here) used to monitor the plasma field and cone sheath potential [15].

Argon gas was fed into a cavity on the outside of the anode. It passed through the center of the thin anode end plate (0.25 mm thickness, with a hole 4 mm in diameter through the center, for the cathode) and along the length of the sample cathode. Gas was carried downstream, via an electrically insulated “feed through” in the source housing, through a sliding gate valve, opening out to a 25-mm-id pipe work and to a rotary pump (Edwards, E2M18). The size of the outlet at the source set an upper limit to the attainable flow speed at  $\sim 10 \text{ m s}^{-1}$ . A liquid nitrogen cold finger was used to prevent backstreaming of the rotary pump oil.

Flow rates in the range of 20–500 cubic centimeter per minute at STP (SCCM) were controlled manually using a needle valve and monitored by a mass flow meter (Tylan General, FM-260). A partial opening of the gate valve acted as a manual throttle to the gas flow and allowed independent control of the source pressure and flow rate. The source pressure was monitored using the ion-gauge (VC200, MSS Ltd.) pressure in the source housing. The source housing ion-gauge pressure rises due to the escape of gas, mainly through the ion exit orifice. The response was calibrated against the actual source pressure using a capacitance manometer (MKS Baratron, type 122A) connected to the outlet from the source, outside the source housing, keeping the gate valve closed. This avoided inaccuracies in pressure reading due to the pressure gradient or caused by the Venturi effect when the gas flow speed was high. The pressure readings quoted in these experiments are therefore a measure of the source pressure at the sampling orifice. As the source is used, the orifice slowly gets blocked by condensation of the cathode material and this affects the calibration. It was important to check this at regular intervals to ensure that changes were not significant.

The background pressures in the source housing and analyzer sections were  $< 10^{-7}$  Torr. The working background pressures reached about  $1 \times 10^{-4}$  Torr and  $1 \times 10^{-6}$  Torr, respectively, with 4 Torr of Ar in the flow source. To avoid significant scattering effects on the ion beam, the pressure range examined was restricted to 3 Torr in the source.

The source floated at 4000 V with respect to the source housing, which was at earth potential. To avoid the possibility of accidental discharge to the source rotary pump, it was mounted on an insulating board, and the power fed through its own isolation transformer, floated at the same voltage.

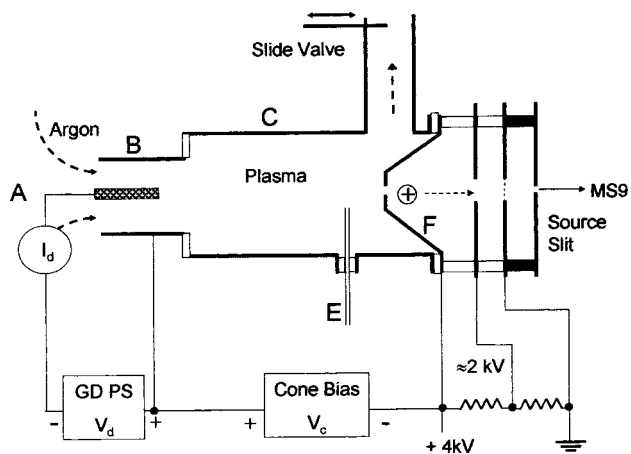


FIG. 3. Schematic of the FFGD ion source and electrical connections: GD PS, glow discharge power supply unit;  $V_d$ , discharge voltage;  $I_d$ , discharge current, and  $V_c$ , cone bias voltage.

The source gas supplies were protected from “flash over” by fitting isolating (10 kV) ceramic feed throughs into the high pressure side of the gas line, close to the flow meter.

### B. The static glow discharge source

This source and its operation were described before [16]. A pin shaped sample cathode, as above, protruded into a cylindrical cavity 12 mm in diameter and 11 mm deep. The ion exit plate blocks off the opposite end of the cylindrically shaped cell and also forms the anode. The body of the cylinder was left electrically floating. Gas entered through the side wall and escaped only via the 0.5-mm-diameter ion exit hole. Therefore, it had a relatively long residence time in the source (hence the epithet “static”). Pressure was measured by a pressure transducer via a connecting pipe on the opposite side. While the distance through the aperture was 0.25 mm as for the FF source, the surface area was 2.8 times larger. The end of the pin was a distance of about 5 or 6 mm from the ion exit aperture. The source was used with the same mass spectrometer and similar ion optics to the FF source.

### C. The mass spectrometer

The apparatus was constructed by modifying a reconditioned MS9 instrument (originally built by AEI Ltd., with a modernized electronics console by MSS Ltd., both of Manchester, England). This was a high-resolution double-focusing mass spectrometer, of “Nier-Johnson” geometry, with modifications similar to those described earlier [16]. The differentially pumped probe inlet was mounted on the source flange, coaxial with the source. A pair of beam-centering plates ( $G$  in Fig. 2) were mounted at a distance of 6 mm from the base of the ion exit cone and 6 mm from the earth plate, which was 11 mm from the *source slit* (at the first focal point of the mass spectrometer). The total distance from the ion exit aperture to the source slit was 42 mm.

The electrical arrangements are shown in Fig. 3. The homebuilt GD power supply provided up to 1500 V at a maximum current of 5 mA. The cone floated at the acceler-



TABLE I. Potentials measured relative to the flowing Ar/Cu plasma (pressure is 2 Torr,  $V_d=500$  V);  $\pm$  numbers in brackets represent the limits of variability.

Gas added	Residence time ( $\pm 0.1$ ) (ms)	Id ( $\pm 0.01$ ) (mA)	Cone bias $V_o$ ( $\pm 0.01$ ) (volt)	Wall $V_{E,\text{wall}}$ ( $\pm 20$ ) (mV)	Field $V_{DE}$ ( $\pm 40$ ) (mV)	Sheath $V_{EF}$ ( $\pm 30$ ) (mV)
None	9.2	1.54	0	-160	+200	+2200
None	6.7	1.92	0	-200	+200	+400
None	4.6	2.58	0	-200	+80	+200
0.1% He	4.6	2.63	0	-250	+100	+250
1.0% H <sub>2</sub>	4.6	2.48	0	-180	+100	+350
None	4.6	2.63	-5.5	-250	-100	-5000

ating voltage (HT) of the mass spectrometer, which was set at 4 kV [17]. Ions emerging from or created at the aperture were therefore accelerated to an energy of 4000 eV before passing through the mass spectrometer. The anode side of the GD supply could be floated at a positive voltage with respect to the cone, which was thus biased relative to the anode at a selected voltage between 0 and -110 V. In other experiments it was possible to apply a positive bias [18]. All supplies were powered via a single isolation transformer floated at HT. Intermediate voltages applied to the beam-centering plates were supplied by the mass spectrometer console and served to both focus the ion beam and guide it towards the source slit. The field generated between the cone and the beam-centering plates was a maximum of  $2000 \text{ V cm}^{-1}$ . It is likely that the field inside the cone, as first encountered by particles leaving the aperture, was less.

Data were collected from meter readings or using a fast recorder during full scans. Masses were identified by a voltage from the Hall probe inserted between the poles of the magnet and calibration was carried out, if necessary, using a sample pin of multiple twisted wires of different metals (e.g., Al, Fe, Cu, Ag, Wn, Au, and Pb). While small changes in the relative ion signals did occur when the focusing conditions were changed, the major effects reported here were independent of focusing conditions.

#### D. Secondary gas additions

H<sub>2</sub> and He gases were titrated into the flowing plasma, without further purification, via a needle valve and flow meter through *E*, at a point  $>30$  mm downstream from the cathode fall. The gases therefore did not interact with the cathode fall and negative glow regions under the experimental conditions used in these experiments. The gas entered the plasma perpendicular to the flow from both sides of the flow tube simultaneously and in the plane perpendicular to the direction of the gas outlet. Any hydrodynamic effect was discounted by the fact that adding He, even in quite large quantities (up to 10% of the main flow gas), neither had any significant effect on the recorded mass spectra, nor did it affect the plasma potential.

#### E. Materials

Source parts were constructed from nonmagnetic stainless steel (316), PTFE™, PEEK™, or Vespel™. Spacers and in-

ulators in the high vacuum region were made from accurately ground quartz glass. Cu (99.95%) was from Goodfellow Metals Ltd. Cambridge, England. Gases were research grade (Ar 99.9995%, H<sub>2</sub> 99.999%, and He 99.9995%) from BOC, UK Ltd. and used without further purification. Argon carried a stated water impurity of  $<4$  parts per million by volume.

#### F. The FFGD source in operation

In operation, *B* of Fig. 3 is the anode, *F* is biased relative to *B*, and *C* is left floating. The plasma extends down the flow tube, although the bulk of the discharge occurs across *A* and *B*. For example, with an Ar flow rate at 400 SCCM, source pressure of 2 Torr,  $V_d$  set to 500 V,  $I_d$  was 2.7 mA [19], but the current to the sample cone (when held at anode potential) was only in the range of 100–130  $\mu\text{A}$ . The flow speed under these conditions was  $8.6 \text{ m s}^{-1}$  and the residence time of the plasma in the flow tube was therefore  $4.7 \times 10^{-3} \text{ s}$ . The plasma behavior can be sensitive to surface conditions. To ensure reproducibility, starting with a fresh cathode pin, the sputtering discharge was run for at least 1 h prior to commencing the experiments. The surfaces in touch with the plasma were therefore always freshly deposited with Cu. The reproducibility was also sensitive to the lifetime (and hence the surface area) of the cathode pin. Conditions were reproducible to within 5%, day to day, provided fresh cathode pins were used.

Because the pumping port is to one side, the plasma flow at the sampling aperture was offset from the center, as evidenced by the asymmetrical “burn” mark on the cone (visible after recent cleaning, but which then gets obscured by Cu deposition). This favored the pumping side of the source by 1 or 2 mm.

There were four independent variable parameters affecting mass spectra generated by this source. These are the discharge voltage  $V_d$ , the source pressure  $P$ , the cone bias voltage  $V_c$ , and the volume flow rate  $F_{\text{gas}}$ . The discharge current  $I_d$  was dependent on  $V_d$ ,  $P$ ,  $F_{\text{gas}}$ , and on the sample geometry. The average temperature of the source flow tube, as measured by a Pt resistance thermometer (Hereaus Pt100 class A, TC Ltd. Uxbridge, UK) closely fitting into a hole drilled into the 10-mm-thick wall, close to the cone, reached a steady state 40–45 °C under the usual operating

conditions ( $V_d=500$  V,  $I_d=2-3$  mA,  $P=2$  Torr, and  $F_{\text{gas}}=200-400$  SCCM).

Digital voltmeters (Beckman Industrial, DM78) and Keithley (model 602) electrometers were used in a potentiometric circuit to monitor the zero current potentials [20] between  $D$  and  $E$  ( $V_{DE}$ ) and between  $E$  and  $F$  ( $V_{EF}$ ), of Fig. 2, reported in more detail elsewhere [15].  $D$  and  $E$  were 20 and 8 mm upstream from the cone. This gave measures of changes to the field through the flowing plasma, and the sheath potential at the sampling cone aperture. Typical values are given in Table I. The  $\pm$  numbers in brackets represent the limits to the degree of instability encountered during the measurement. The zero current voltages between  $D$ ,  $E$ , and  $F$  were self-consistent. The current at the cone surface was also measured on some occasions.

### III. RESULTS

#### A. Copper atom density in the plasma

A copper cathode was chosen for the work described here because it is readily sputtered, is often used in studies of fundamental glow discharge processes [1], and it was used before [5]. The copper atom density in the plasma was estimated approximately from the net erosion rate of the cathode, measured by its weight loss. This value, corrected for changes in the discharge current, was found to increase from the static gas value, in direct proportion to the gas flow speed, keeping all other parameters constant [21]. The static gas value is due to diffusion from the cathode to the walls of the surrounding anode [22]. The extra weight loss when the gas is flowing is that transported by the flow, giving the Cu atom flow rate. There will be losses due to radial diffusion as it flows down the tube. The derived plasma concentration is therefore an upper limit, which lies closest to the actual value at the shortest residence times. With a flow speed of  $\approx 9$  m s $^{-1}$ , a pressure of 2 Torr, 500 V discharge voltage, and 2.8 mA of discharge current [19], the Cu atom flow rate into the extended plasma was  $\approx 2 \times 10^{15}$  atoms s $^{-1}$ . Hence  $[\text{Cu}]_{\text{gas}}$  was  $< 4 \times 10^{11}$  atoms cm $^{-3}$ , compared with the argon gas density at  $3 \times 10^{16}$  cm $^{-3}$ .

#### B. Comparison of mass spectra between static and fast-flow sources

Examples of mass spectra obtained from the FFGD and static GD sources, using a copper pin cathode, are shown in Fig. 4. Only ions  $\geq 1\%$  of the most abundant are shown. Spectra were dependent on the source conditions, however, over a very large range of conditions the FFGD and static source spectra were significantly different in two respects, shown by Fig. 4. First, the general sensitivity towards the cathode species is much greater for the flowing source and second, the background ions due to the discharge gas and its impurities (such as air and water) are much reduced from that of the static source. The FF source consistently gave a  $\text{Cu}^+$  signal that was larger by a factor  $>50$  for the same sample size, discharge power, and gas pressure when the two sources were otherwise optimized for the best  $\text{Cu}^+$  signal in each case, and after allowance for the different diameters of

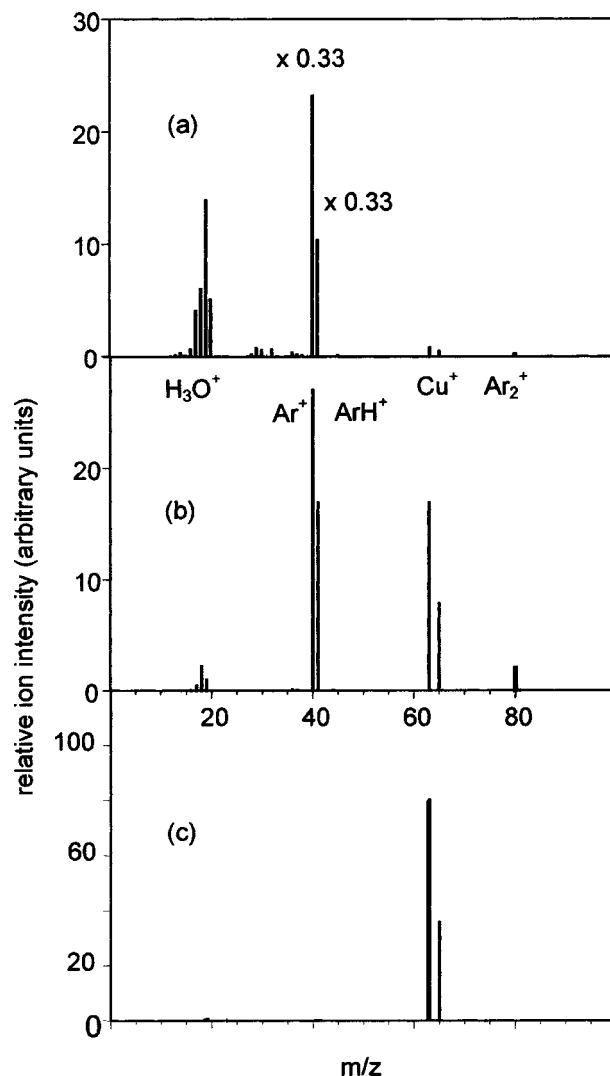


FIG. 4. Comparison of mass spectra produced from (a) the static GD ion source ( $V_d=600$  V,  $I_d=2.0$  mA, pressure adjusted for optimum  $\text{Cu}^+$  signal); (b) the FFGD ion source ( $V_d=509$  V,  $I_d=2.91$  mA,  $P=2$  Torr,  $V_c=-100$  V, and  $F_{\text{gas}}=450$  SCCM, giving a flow speed of  $\sim 10$  m s $^{-1}$ ), both attached to the modified MS9 mass spectrometer; (c) the FFGD source, but with  $<0.3\%$   $\text{H}_2$  gas leaking into the flowing plasma at point  $E$  [509 V, 2.91 mA,  $V_c=-100$ , 2 Torr, 425 SCCM (cubic centimeters per minute at STP)].

their sampling apertures. The signal from the flowing source continued to increase with gas flow speed; there is therefore still room for improvement in terms of increasing the absolute cathode ion intensity in the spectrum, for otherwise constant discharge conditions.

As before [5], the main ions in the spectra of both sources were those normally [23] detected from an argon (copper) glow discharge, i.e.,  $\text{Cu}^+$ ,  $\text{Ar}^+$ ,  $\text{ArH}^+$ ,  $\text{Ar}_2^+$ ,  $\text{H}_2\text{O}^+$ , and  $\text{H}_3\text{O}^+$ . They are the result of ionization not only of the discharge gas but also water-derived peaks (impurity in the gas supply and degassing from the walls). When fully optimized,  $\text{Cu}^+$  can be the base peak in the FFGD spectrum [24]. This compares with the static source, in which  $\text{Cu}^+$  is usually  $<10\%$  of the base peak (normally  $\text{Ar}^+$  or  $\text{ArH}^+$ ) [16].

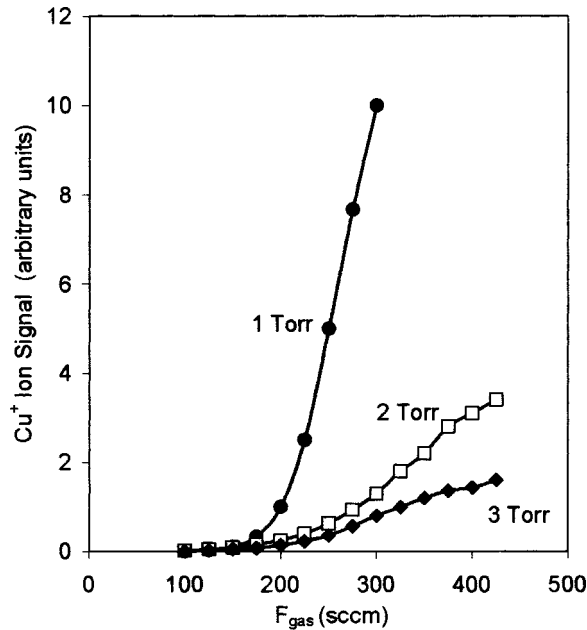


FIG. 5. Variation of  $\text{Cu}^+$  signal with flow rate of discharge gas at different source pressures, keeping cone bias constant at  $-5.5$  V.

In the FFGD mass spectrum, although ions of the discharge gas and molecular ions were present, they were in much lower abundance, giving a comparatively clean spectrum. A flowing gas GDMS study by others [25] also reported very low background interference from molecular ion formation.

**C. Dependence of ion intensities on discharge power, pressure, and flow rate**

Increasing the power of the GD, but keeping all other parameters constant, increased the ion signals (as expected and therefore the data is not shown) because both the ionizing discharge current and the cathode sputtering energy (and therefore the rate of sputtering) increase as the discharge voltage goes up. Figure 5 shows how the detected  $\text{Cu}^+$  ion intensity varies with flow rate for different fixed pressures at constant discharge and cone voltages. In the range studied, greater sensitivity was achieved at lower pressures, with copper ions continuing to increase up to the maximum flow rate possible. The main reason is the increased transport of sputtered material towards the cone. A general increase in the efficiency of ions detected also occurs at the faster flow. Figure 6 shows how the discharge current increases with increasing  $F_{\text{gas}}$  for a fixed discharge voltage and pressure. It also shows detected ion signals, normalized by division by the discharge current. In a steady state glow discharge the rates of ion and electron production must balance, and the expectation would therefore be that the normalized  $\text{Ar}^+$  signal should not change, if it represented the free-ion concentration in the plasma. The significant increase of this parameter as the flow speed increases suggests that it reflects something different.

The pressure effect is complex. Increasing pressure leads to increased ionization (and hence increased discharge cur-

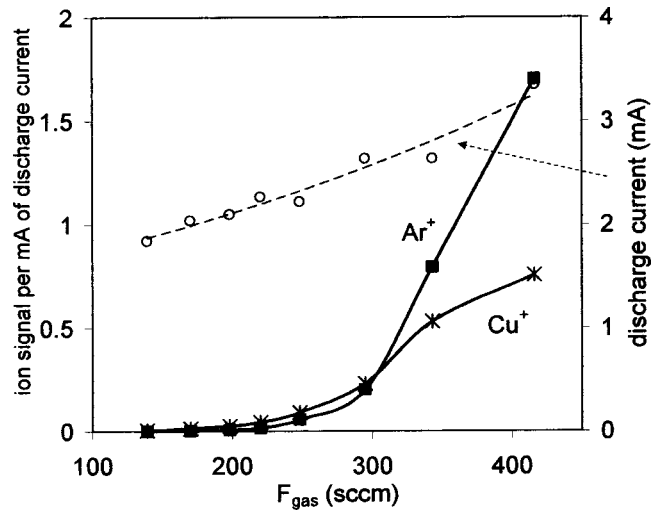


FIG. 6. Variation of ion signals ( $\text{Ar}^+$  and  $\text{Cu}^+$ ) with gas flow rate, normalized with respect to the changing discharge current (also shown), keeping  $V_d$  (500 V),  $P$  (1.75 Torr), and  $V_c$  ( $-5.5$  V) constant.

rent). On the other hand, it causes a reduction in the net sputter yield [22]. Also, for a given flow rate, the gas speed decreases with increasing pressure [5]. The combined effect on processes leading to detected ions will also be complicated by formation and removal processes in the gas phase. In optimizing the cathode ion signals, the increased sputtering of the sample into the plasma must be balanced against the timing required to optimize gains and losses in the reaction tube. The optimum pressure was  $\leq 1.5$  Torr.

**D. Dependence on the cone bias voltage**

Figure 7 shows the variation of  $\text{Cu}^+$  and  $\text{Ar}^+$  intensities with increasing cone voltage, at fixed pressure and discharge

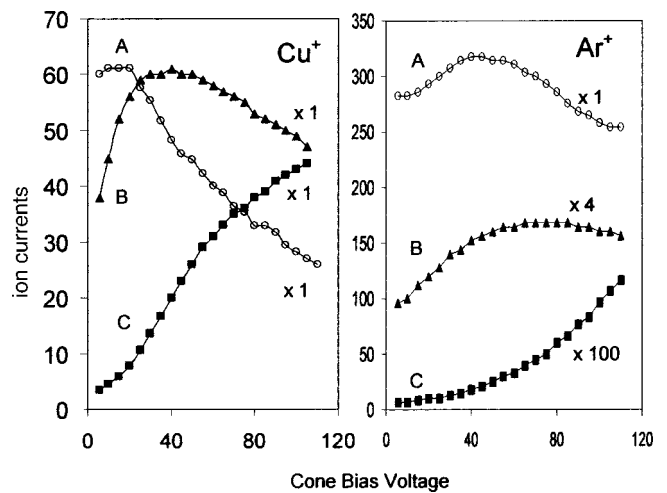


FIG. 7. Variation of ion currents (arbitrary units) for (a)  $\text{Cu}^+$  and (b)  $\text{Ar}^+$ , as  $V_c$  was varied, keeping  $V_d$  (533 V),  $I_d$  (2.67 mA), and  $P$  (2 Torr) constant, for different constant flow rates:  $F_{\text{gas}}$  (SCCM) and plasma residence time in the flow tube ( $10^{-3}$  s units), respectively, are given in brackets: A (425,4.3), B (300,6.3), and C (200,9.3).

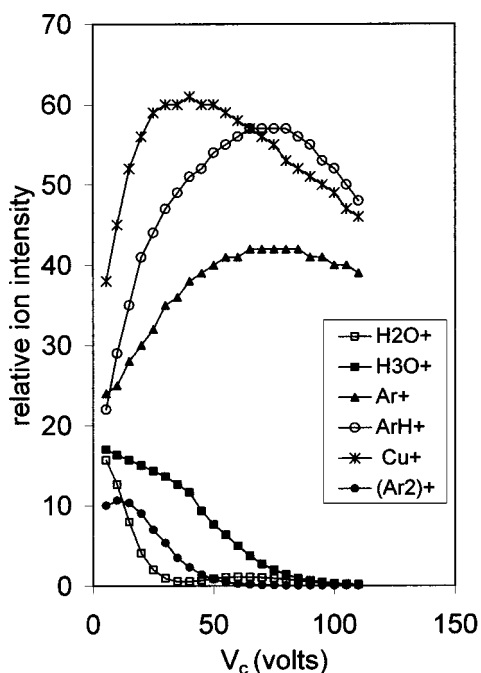


FIG. 8. Ions in the mass spectrum from the 6.3-ms plasma; signal intensity variations with changing cone bias, keeping constant:  $V_d$  (533 V),  $I_d$  (2.67 mA),  $P$  (2 Torr), and the flow rate.

voltage, for differing fixed rates of flow. This indicates that, at the fastest flow speeds in our instrument, the ion signals are highest at the lowest cone voltages. At low flow speeds the signal rises with the increasing cone bias as expected, but with a sluggish response. At intermediate flows the signal goes through a maximum. Figure 8 shows variations for all the main ions from the 6.3-ms plasma.

#### E. The addition of hydrogen gas to the flowing plasma

Additions of  $H_2$  (<0.1% of main flow) titrated into the downstream plasma led to a significant “cleanup” of discharge gas ions in the spectrum and boosted the  $Cu^+$  signal, see Fig. 4(c), as before [5]. This happens over the full range of cone bias voltages applied (see Fig. 9). Although technically difficult with our present apparatus, the negative ion spectrum was also measured, both with and without  $H_2$  present. In pure Ar, the most abundant ion detected was  $OH^-$  (from the trace water), as expected and with low intensity. When  $H_2$  was added, the  $H^-$  signal produced [26] was a factor of 300 lower in intensity than any cautions and therefore negative ion formation was not a significant factor in the chemistry.

The wall, plasma field, and sheath potentials,  $V_{E,wall}$ ,  $V_{DE}$ , and  $V_i$ , were also monitored during the addition of  $H_2$ . Results are shown in Table I. There was a net negative current through the plasma to the cone when  $V_c$  was biased at the anode voltage. Figure 10 shows how this was quenched when  $H_2$  was titrated into the plasma.

### IV. DISCUSSION

#### A. The positive column character of the fast-flow plasma

The ion exit of the static source was 5 or 6 mm from the end of the cathode pin and was therefore in contact with the

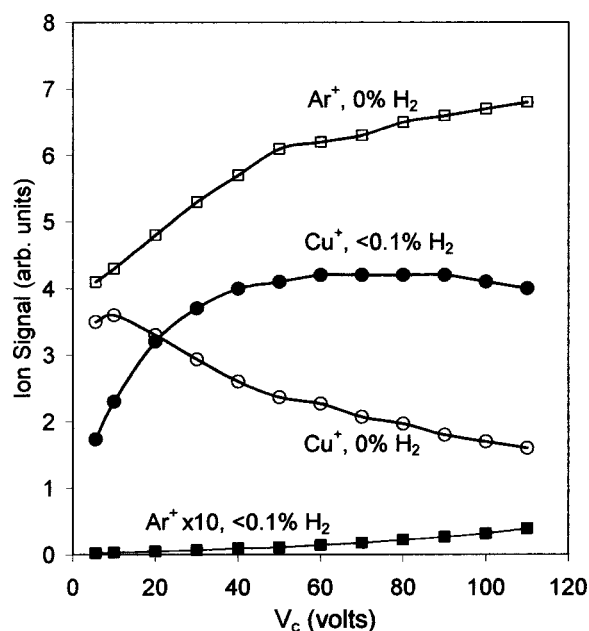


FIG. 9. Effect of adding  $H_2$  into the flowing plasma at different values of cone bias; the graph shows the variation of  $Cu^+$  and  $Ar^+$  signals with  $V_c$ , with and without titrating  $H_2$  (<0.1% of the total flow) into the flowing plasma through gas inlet  $E$  of Fig. 2, keeping constant:  $V_d$  (536 V),  $I_d$  (3.36 mA),  $P$  (1.75 Torr), and  $F_{gas}$  (372 SCCM, gas flow speed is  $9.20 \text{ m s}^{-1}$ ).

negative glow. The distance in the fast flowing source was  $>40 \text{ mm}$ . Since the plasma density reaching the cone must depend on the balance between formation and removal processes, it had been thought that the fast flow might “stretch” the negative glow region in space onto the sampling cone by reducing the plasma residence time. Although they became less positive as the residence time of the plasma decreased,

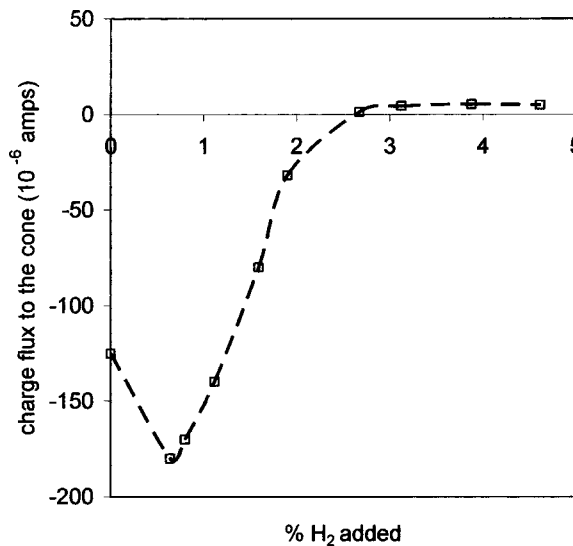


FIG. 10. Electron current to the cone as a function of  $H_2$  added into the flowing plasma, close to the cone;  $V_d=500 \text{ V}$ ,  $I_d=3 \text{ mA}$ ,  $V_c=0 \text{ V}$ ,  $P=2 \text{ Torr}$ , residence time being 4.3 ms;  $H_2$  was added 2-mm downstream of the cone aperture when the reaction was 20 times less sensitive than addition through  $E$  (see text).



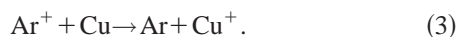
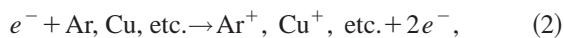
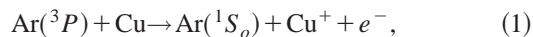
$V_{DE}$  and  $V_s$  were always positive. The plasma therefore had the character of a positive column. The current flow through this section of the plasma was 100–130  $\mu\text{A}$ , compared to the total discharge current of 2.6–2.7 mA, the majority of which discharged across the much shorter distance of 3.8 mm between *A* and *B*.

## B. The formation of ions in the FFGD mass spectrum

### 1. Conventional model

When electrons leave the cathode of the GD, they are accelerated across the cathode fall (a distance of ca 1 mm at a pressure of 2 Torr) into the negative glow (see Fig. 1), where the major part of the ionization occurs. The negative glow extends over a greater distance and in the idealized plasma it is a field-free region. The net effect in the discharge is for each ionizing electron to create an  $\text{Ar}^+$  ion and an extra electron. It is the ions and electrons, slowed down by collision, which create the plasma between the cathode fall and the anode.

This complex medium contains a very large population of excited neutral species, in addition to ions and is a good source [27] of argon metastable atoms in their first excited state,  $(3p^5 4s^1) ^3P_{2,0}$ . These are formed either directly, by electron impact, at the cathode fall or negative glow boundary, or in the plasma itself as a consequence of an energy transfer cascade, by radiative or collisional quenching of higher excited states. The most important ionization process contributing to the metal cathode cationic signal is therefore considered to be Penning ionization [8,28], as in reaction (1). The contributions of reactions (2) and (3), electron impact [29], and charge transfer [30] have also been considered:



Important removal processes in the plasma are thought to be recombination, diffusion of the ions to the walls of the source, and interfering ion-molecule reactions and these are all used in modeling studies [31].

### 2. Field ionization of excited states

It is usually assumed that ions detected through the anode of the GD are those incident on the aperture. However with a zero bias on the cone ( $V_c=0$ ), the positive field of the plasma and the cone sheath potential (see Table I) will inhibit cautions migrating towards the cone and entering the sampling aperture. If the ions detected do represent ions present in the bulk plasma we would expect the use of a negative bias (i.e., increasing  $V_c$ ) to extract those ions more efficiently. In fact, with the shortest residence time, the opposite happened, as shown in Fig. 7 for  $\text{Cu}^+$  curve *A*. The maximum ion signal occurred when  $V_c \approx 0$ , decreasing thereafter. In the same experiment, the  $\text{Ar}^+$  signal increased a little at first, but then also decreased to below the value at  $V_c=0$ . We conclude from this that the ions detected under these condi-

tions must have been created mainly outside the plasma, from excited state neutral precursors. While the free cations will be inhibited by the positive sheath field, excited neutral precursors will pass through the aperture with the flux of gas.

The ions detected are therefore formed by either autoionization or field ionization in the accelerating region of the mass spectrometer. To be detected efficiently by the mass spectrometer the ions must form almost immediately as their neutral precursors enter the ion accelerating region. This can occur easily and quickly only if the excited neutrals are close in energy to their ionization level, i.e., only if they are Rydberg species. Field ionization also happens to be probably the best method for detection of such species [13,32].

According to theory, the Stark field required to ionize Rydberg atoms is given [32] by

$$E_{\text{Stark}} = c/n^4,$$

where  $n$  is the principal quantum number and  $c$  is a constant. The value  $c = 6 \times 10^8 \text{ V cm}^{-1}$  is quoted in Ref. [32] describing experiments on Rydberg states of Ar ionizing in a background gas of  $1 \times 10^{-5}$  Torr. With a field gradient of up to  $2000 \text{ V cm}^{-1}$  (the voltage on the beam-centering plates, *G* of Fig. 2), the critical quantum number  $n_c$  for ionization would be in the region of  $n_c = 24$ . Only excited atoms very close to or above their ionization level would therefore be ionized fast enough to be detected efficiently by the mass spectrometer. We have reported the presence of autoionizing or field-ionizing states of argon before, but emanating from the static source [33]. Autoionizing states are characteristic of Rydberg atoms that have an excited core electron and an excited valence electron, and whose ionization energy lies above the first ionization threshold [13]. The electron can tunnel through to the first ionization continuum and is automatically ejected.

Ions formed further away from the exit aperture acquire less energy from the accelerating field. It was clear from the asymmetry of the ion-beam intensity, monitored as it passed between two plates in the second field-free region between the electrostatic analyzer and the magnetic analyzer, that substantial quantities of ions are created down-field, soon enough to be carried through the ESA but too late to acquire sufficient energy to transfer through the flight tube of the following magnetic field. This was *not* the behavior observed when using a “chemical ionization ion source,” with the same pressure of argon gas and similar ion optics, in an exactly similar MS9 instrument [33].

Further support for this field-ionization mechanism came from the results of similar experiments conducted with a FFGD source attached to a quadrupole analyzer [21] and discussed in a preliminary publication [10]. The ion-beam accelerating field in a quadrupole analyzer is in the region of a few  $\text{V cm}^{-1}$  at most and therefore too low to induce field ionization efficiently for states below the ionization level, although autoionization might be detected. For the same conditions as employed in the experiments, which provided data for curve *A* in Fig. 7, relatively few ions were detectable in the quadrupole based instrument. However, their detected intensity increased significantly on application of the negative



cone bias; the opposite effect to that seen here [34]. Also, the main ions detected were  $\text{Cu}^+$ , the intensity of which was a factor of 100 greater than  $\text{Ar}^+$  and  $\text{ArH}^+$ .

### 3. The cone bias effect

The voltage probe measurements (see Table I) showed that when the cone voltage is applied, the drop in voltage at the cone is detected on  $E$ , almost in full. It also reverses the field along the plasma, but that field is still very small compared to the applied bias. At the shortest residence times,  $V_{DE}$  was only  $-0.25$  V when  $V_{EF}$  was  $\sim 90$  V. The wall potential with respect to  $E$  also changes relatively little. The applied negative bias therefore does not extend far into the bulk plasma, but creates a sharp negative field immediately in front of the cone [35]. This is expected, based on probe potential measurements in other plasmas [36]. The positive cone current induced was limited to only a few microamperes. According to theory, based on the free ion and electron model plasma, this is caused by the migration of ions from the plasma to the surface, which is rate limiting because of their high mass, relative to that of electrons. It seemed remarkable therefore that ion signals detected in the MS9 instrument should have gone down in intensity, as shown in Fig. 7 for curve  $A$  of the  $\text{Cu}^+$  profiles when  $V_c$  was increased. We would have expected the opposite if the ions were migrating from the bulk plasma. On the other hand, the different profiles of all the curves displayed in Fig. 7 are easily rationalized by using the excited Rydberg state model, as follows.

Rydberg atoms are stabilized in the presence of small fields, but destabilized by strong fields, depending on conditions and the energy of states involved [13]. There are therefore three possible effects of using the negative cone bias: (i) the Stark effect will cause the highest-energy Rydbergs to become dissociated inside the glow discharge cell, before they have time to get out, causing a drop in the ion current created by field ionization outside the source; (ii) ions created this way in front of the cone inside the cell may be pulled through the aperture by the negative field gradient of the cone bias; and (iii) Rydbergs of energies too low to become ionized inside the cell may nevertheless become more excited (*field excitation*) in the sheath field, which in turn will render such ions more liable to field ionization outside the cell [37] and hence could cause an increase in the detected ion signal. The overall changed ion current recorded by the MS9 will therefore be the net result of these three effects, which will depend on the population and energies of species in the plasma (i.e., the residence time, for a fixed discharge voltage and pressure), the field applied to the cone and the efficiency of ion transfer through the aperture.

The highest-energy Rydbergs are the most easily field ionized and these are encountered at the shortest residence times, hence the effect (curve  $A$ ) on  $\text{Cu}^+$ , at 4.3 ms, in which there is a *decrease* in ions recorded as the cone bias is increased because (i)  $>$  (ii) + (iii). At the residence times of 6.3 and 9.3 ms, the average energy and the abundance of Rydbergs will be progressively lower. Thus, we have profile  $C$  for  $\text{Cu}^+$  in Fig. 7 (and indeed for both  $B$  and  $C$  profiles of the  $\text{Ar}^+$  signal) in which the signal increases with increasing

$V_c$ , because (i)  $<$  (ii) + (iii). An interesting situation arises for profile  $B$  of  $\text{Cu}^+$ , which first rises, goes through a maximum (at around  $V_c = 40$ ), and decreases again as the bias is increased. In this situation, the  $\text{Cu}^R$  energies (on an average) are too low to be directly dissociated inside the cell by low applied bias voltages, but are high enough to dissociate at the higher bias voltages. Hence, for  $V_c < 40$  V: (i)  $<$  (ii) + (iii), at  $V_c = 40$ : (i)  $\approx$  (ii) + (iii) and for  $V_c > 40$  V: (i)  $>$  (ii) + (iii). Similar behavior, although less pronounced, is exhibited by  $\text{Ar}^R$  in the 4.3-ms plasma (profile  $A$  of  $\text{Ar}^+$ ).

Further indications that the curves of increasing ion current with increasing  $V_c$  (e.g., the  $C$  profiles) represent more than a simple ion extraction effect are the sluggishness of response at low  $V_c$  values and the considerably different responses of different ions. Ion extraction usually causes a sharp increase followed by a tailing off of response. Here, the initial response is sluggish. In ion extraction most ions behave similarly although there may be an effect due to different masses in favor of lighter ions; here  $\text{Ar}^+$  the lighter ion has a much more sluggish response than  $\text{Cu}^+$ . Since the plasma contains a manifold of different energy states, the  $V_c$  dependence curves are a convolution of four processes: field excitation, field ionization either inside or outside the cell, and ion extraction from the plasma boundary. The response to  $V_c$  will therefore be different for each species of the discharge, since the manifold of Rydberg states created will be different for different atoms and molecules. This is as indicated in Fig. 8.

The plasma becomes more relaxed at longer residence times through reaction, collision, radiation, and diffusion to the walls and so both the plasma density and the average energies of Rydbergs present will decrease. Overall, therefore, detected ion currents drop with decreasing flow speed, as happens between curves  $A$ ,  $B$ , and  $C$  for  $\text{Ar}^+$  in Fig. 7. However, the same relative decrease does not happen to  $\text{Cu}^+$ . While the corresponding  $\text{Ar}^+$  signal decreased by a factor  $> 10$  between curves  $A$  and  $B$ , the  $\text{Cu}^+$  signal remained the same order of magnitude, despite the fact that, at the lower flow speed, there was a decrease in the flow of copper into the downstream plasma (see above).

The reason is a net transfer of energy from the excited states of Ar to those of Cu with its much lower ionization energy (7.73 compared with 15.76 eV for Ar). The net cooling effect on the manifold of high  $n$  excited states of argon (by collisional quenching, etc.) will therefore be much more pronounced than for Cu. As the higher-energy states of Ar become depopulated (and therefore stop being field ionized) they relax down towards the first excited state at 11.5 eV. Having a very long lifetime, this acts as a bottleneck to further energy dissipation leading, at first, to an increase in the lower-energy state populations of Ar, which can more easily transfer energy to excited states of Cu. Therefore, although the Cu atom concentration launched into the flowing plasma is lower at the lower flow speeds, the effect is offset by the increased rate of energy transfer from the lower excited states of Ar. At first, therefore, the  $\text{Cu}^+$  signal stays almost constant as the residence time is lengthened. A similar, but more pronounced, effect is observed when  $\text{H}_2$  is added to the fast-flowing plasma and is discussed in more detail below.

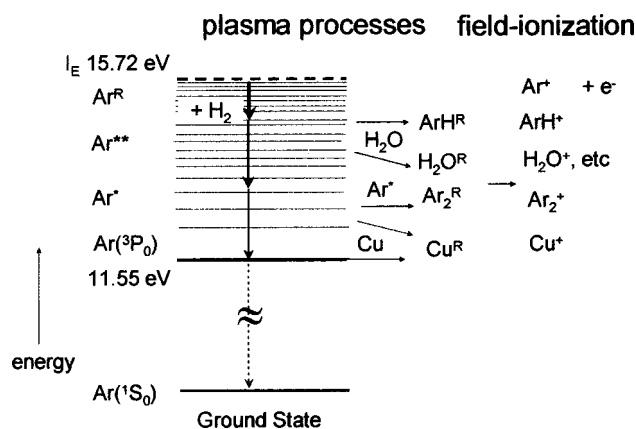


FIG. 11. Schematic representation of the excited state model of the flowing plasma, indicating a manifold of excited states of Ar up to its ionization level, and energy transfer processes leading to the formation of Rydberg species which become field ionized as they enter the accelerating region of the mass spectrometer.

### C. Hydrogen reactions at the boundary

The afterglow plasma model, as given previously [5], is represented in Fig. 11. The lowest excited energy states of Ar ( $4s, ^3P$ ), are produced in abundance in the discharge [27] and are widely accepted as a principal reagent [8] in the ionization of metal atoms in the plasma. According to the excited state model, many of these lower excited states of Ar are populated by radiative or collisional energy transfer from high-energy neutrals in the bulk plasma. The latter are also the precursors to discharge gas ions in the mass spectrum. The fast quenching of the higher states of Ar by  $H_2$  serves to depopulate these, while populating lower excited states that are closer in energy to the excited states (including autoionizing states) of copper. The increased  $Cu^+$  signal then comes from increased interaction of Cu atoms with lower-energy excited state products of the  $H_2$  reaction. It is possible that product excited states of  $H_2$  are also involved.

In the original experiment, the  $H_2$  entered the flow a few millimeter downstream of the cone aperture and to the side opposite the gas exhaust. It therefore had to diffuse back into the plasma boundary to have an effect. In the current series of experiments the gas was introduced 8 mm upstream of the cone aperture. The same effect occurred, except that the gas flow required to achieve it was a factor of 20 times less. Examples of the results of this experiment are shown in Figs. 4(c) and 9.

The plasma potentials were not previously measured. The changes to the field, sheath, and wall potentials caused by adding  $H_2$  in the current experiments were found to be very small in absolute terms (see Table I), and show that the changes in the mass spectra are therefore not simply caused by changes to the sheath potential. The intensities of  $H^+$ ,  $H_2^+$ , and  $H_3^+$  recorded in these experiments were also  $<1\%$  of the most intense ion peak of the spectrum before  $H_2$  addition and the  $H^-$  intensity was  $<0.4\%$  of the positive ion currents. These observations, combined with the loss of discharge gas atomic and molecular ions, confirm that ion-

molecule reactions are not a significant feature of the loss mechanism, as concluded previously [5].

If free ions (of Ar) and electrons were involved, reaction (4) ought to occur,



since it is very fast [38], followed by reaction (5) which is 100 times faster still [12]. Schram and co-workers [12] have argued that it is this sequence which leads to the quenching of charge observed in  $H_2/Ar$  plasmas. However, for complete quenching of the free ions we would have expected the wall potential to be nullified and for the positive sheath potential to rise significantly as it did just by increasing the plasma residence time to 9.3 ms (allowing more time for plasma decay by diffusion and collisional losses). When sufficient  $H_2$  was added to completely quench the discharge gas ions in the mass spectrum, the wall potential changed by no more than 50 mV and the sheath potential increased by only 150 mV. This compares with 2200 mV caused just by increasing  $\tau$  to 9.3 ms (and *without* adding  $H_2$ ). The small changes induced by the  $H_2$  additions are therefore inconsistent with the recombination mechanism.

In addition, when a large ion extraction voltage is applied, it should help separate out the ions from the electrons at the boundary and allow the ion-molecule reaction to be detected. As shown in Figs. 4(c) and 9, even at high negative cone bias voltages, the addition of  $H_2$  still causes the discharge gas ions to disappear from the spectrum, including  $ArH^+$ , while  $Cu^+$  is still boosted. A further point is that, without any  $H_2$  addition, both  $ArH^+$  and  $H_3O^+$  are detected in abundance due to the presence of trace water impurity. All molecular ions have recombination coefficients which are 100 to 1000 times more efficient than atomic ion-electron recombination [39]. The “recombination” argument above should therefore also apply to these ions. This would cause molecular ion intensities, emerging from a conventional plasma, to be  $\geq 10$  times *lower* than the abundance of  $Ar^+$  [40]. This is clearly not the case [see also the results from the static source in Fig. 4(a), in which  $Ar^+/ArH^+$  ratio was  $\approx 2$ ]. Once more the conclusion is that the ions observed are field-ionized or autoionizing Rydberg species.

As expected (since  $H_2$  is already known to quench charge overall [12]), we find that adding  $H_2$  suppresses the ability of the fast-flow plasma to conduct an electric current (see Fig. 10) from the cathode to the cone. Rydberg atoms have a very high cross section for charge transfer [13]. We propose that a rapid charge transfer across the excited state population is the mechanism for conducting electrons through the flowing plasma across to the cone. The fact that the sheath and wall potentials remain relatively unaffected suggests that the reaction of the  $H_2$  is selective. Excited state chemistry has been used to explain the results of studies of the  $H_2$  effect (as a premixed  $Ar/H_2$  gas in a static GD) in optical emission systems, in which the main effect observed was selective quenching of emitting states [41] (it should be noted that

detectable emitting states in a GD are generally not Rydberg states, because their optical transition probabilities are very low).

#### D. Rydberg atom lifetimes in the plasma

Ar Rydberg states have been much studied in low pressure systems. They can be formed by both electron impact and recombination [32]. Optically accessible states have been studied by laser excitation combined with the technique of zero-electron-kinetic-energy spectroscopy. Longlived states are subsequently populated by collisional angular momentum transfer or the Stark effect and subsequently detected using pulsed field ionization [42]. A surprising observation of all these studies is that the lifetimes of Rydberg states of Ar are much longer than what the current theory predicts, being up to several tens of microseconds as measured by the latter technique. Schiavone *et al.* [43] have measured lifetimes  $>10^{-4}$  s for  $\text{Xe}^R$  states formed by electron impact and recombination. We reported [44] an observation of  $\text{Ar}^R$  states emanating from the negative glow of a static dc glow discharge with dissociating lifetimes in the region of  $10^{-5}$ – $10^{-4}$  s. Experimental results and theory are therefore at odds and the experimental results themselves are often contradictory [45]. Nevertheless, the consensus is that the lifetimes are extended by  $l$  and  $m_l$  mixing (angular and magnetic quantum numbers of the electronic excited state). The high  $l$  and  $m_l$  values, created from low angular momentum states by low electric fields and collisions make these states less optically accessible and hence more stable. At the same time, high fields and energetic collisions can destabilize these states. There is therefore a fine balance and presently experiment seems to lead theory.

The experimental conditions of the previous lifetime studies have all been of comparatively isolated Rydberg atoms (e.g.,  $5 \times 10^{-5}$  Torr [43]) relative to our experiments. The pressures and excited state densities in the present experiments are very much higher and the properties of Rydberg atoms in such a dense medium do not appear to have been quantitatively studied before (although it was suggested long ago that the stabilization processes discussed above should apply in plasmas and discharges [46] and the original evidence for Rydberg species was provided by emission spectra from electrical discharge plasmas).

The ions detected in our experiments are the product of excited neutral species, auto-ionizing or field ionizing as they enter the accelerating region of the mass spectrometer. To undergo efficient dissociation, their energy must be close to the ionization level. The average energy of free electrons in a classical low power dc glow discharge plasma is estimated to be  $\approx 2$  eV in Ar gas at 1 mTorr [1]. At the pressure of 1–2 Torr of the current experiments, collisional cooling will ensure that electron energies are very much less and therefore insufficient to create these states by electron impact in the plasma itself. If formed directly by electron impact, they would have to be formed at the negative glow or cathode fall boundary. It is more probable that they are formed in reaction (6) by recombination:

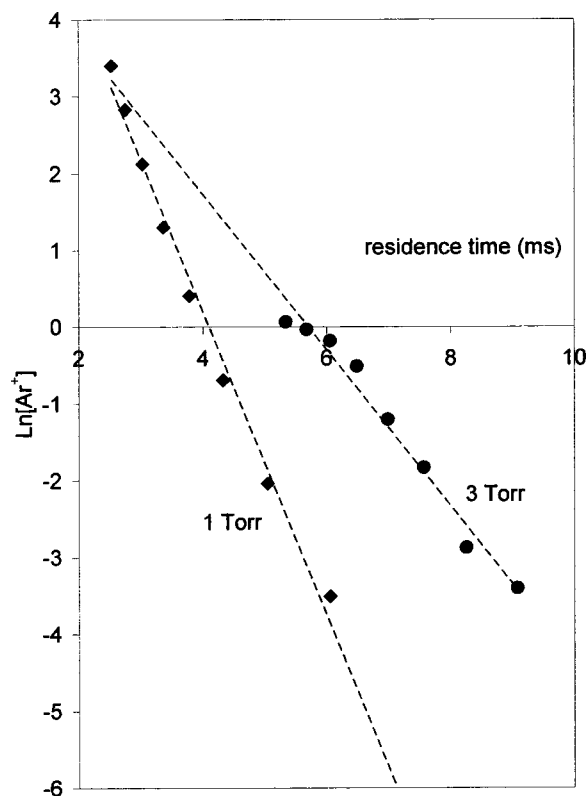
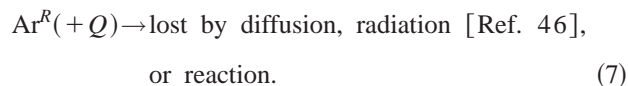


FIG. 12. First-order plot to estimate the lifetime of Rydberg atoms of Ar in the flowing plasma, at two different pressures (shown);  $V_d$  (560 V),  $I_d$  (2.4 mA), and  $V_c$  ( $-5.5$  V) were kept constant.

This could happen in the negative glow or as the plasma is carried down the flow tube. However, even at the fastest flow rates studied here,  $\text{Ar}^+$  did not appear to exist in significant quantity as the free ion, nor was there any evidence for the products of its ion-molecule reactions, by the time the plasma had reached the sampling cone. This was shown above by the effect of the cone bias on the ion signals and the effect of adding hydrogen, which quenched all discharge gas ions even in the presence of a substantial negative cone bias potential. Therefore by the time the plasma had reached the sample cone, it had become almost completely reduced to a Rydberg gas. Since Rydberg species were no longer being formed by reaction (6), we were simply monitoring their decay by reaction (7):



$Q$  is a reactant or quenching molecule. The phenomenological lifetime of the Rydberg atoms in the plasma can therefore be estimated from the change in detected  $\text{Ar}^+$  signal with residence time in the plasma.

Making the reasonable assumption that  $[\text{Ar}^R] \ll [\text{Ar}]$  and  $[Q]$ , the change in  $\text{Ar}^+$  intensity, at constant pressure in the flow tube, should be pseudofirst order. The straight line plots of  $\text{Ln}(\text{Ar}^+)$  versus residence time shown in Fig. 12 are therefore consistent with the model.



Possible sources of error were considered. Under the conditions of these experiments the change in the discharge current was  $<10\%$  over the range of flow speeds used, so that changes to the rate of formation of the excited states due to electron impact and recombination close to the cathode fall are not likely to be significant. The Cu atom density in the plasma does change, increasing linearly with increasing flow speed. If this has an effect on the  $\text{Ar}^R$  density, the higher rate of reaction at the shorter residence times due to the increased Cu atom density will be offset by the increased reaction time at the slower flows. In any case the evidence above indicates that Cu is much more reactive with lower<sup>1</sup> energy states of Ar than the higher states. Another effect to consider is that as the flow speed goes down the sheath potential goes up (0.2  $\rightarrow$  2.2 V). However, this is offset here when the experiments were performed at a constant bias of  $-5.5$  V. In addition, the change in  $\text{Ar}^+$  signal caused by decay mechanisms is very much greater than the effect of the cone bias, as shown by the data for  $\text{Ar}^+$  in Fig. 7.

Lifetimes ( $=1/k$ , where  $k$  is the rate constant for decay of  $\text{Ar}^+$  signal with time) of  $5 \times 10^{-4}$  s at 1 Torr and  $1 \times 10^{-3}$  s for the much lower intensity signals at 3 Torr, are obtained. Similar values were obtained when, instead of using  $\text{Ar}^+$ , detected outside the cone, we monitored the changing electron flux from the cathode to the cone (with  $V_c$  set to 0). This is consistent with our contention that the electron flux to the cone is carried by a sequential charge transfer mechanism through the Rydberg gas. The current carried by this mechanism would be proportional to the concentration of conducting Rydberg atoms at the surface. The values represent a convolution of many different states since the number and degeneracy of high  $n$  and  $l$  Rydberg states is very high.

This result is important since it indicates that lifetimes of Rydberg states of Ar inside the plasma may be an order of magnitude larger than outside. In the collisional environment of the plasma, an increased stabilization of the higher- $n$  Rydbergs in the collisional environment could arise, at least partially, from the loss of entropy if  $n$  decreases (the number of degenerate states is roughly halved for each change of  $n$  by 1). It also indicates that the lifetimes of Rydberg atoms are long enough to play an important role in the mechanism sustaining these relatively high pressure discharges.

### E. Comparison with the static source

The static source also yields copious ions. However the spectrum, when connected to the MS9, is completely dominated by  $\text{Ar}^+$  and  $\text{ArH}^+$  ions. In absolute terms, the  $\text{Cu}^+$  signal is a factor of  $>50$  less than obtained from the FFGD source, under otherwise similar conditions.

Since the ion exit is probably immersed in the negative glow region, the signal may be dominated more by the escape of free ions. However, we have detected Rydberg atoms previously from this source using ion kinetic-energy measurements [33]. These states were found to have lifetimes in

the range  $(0.1-1) \times 10^{-4}$  s, once released into the accelerating region. Since the energy of species in the plasma close to the cathode region is likely to be higher than in the flowing positive column, the abundance and average energy of Rydberg states leaving the plasma are also likely to be higher. They will therefore be more readily field ionized, or indeed may be autoionizing, leading to the very much higher  $\text{Ar}^+$  and  $\text{ArH}^+$  signals, as observed.

The  $\text{Cu}^+$  ion signal is much greater in the fast-flow source for three reasons. The fast flow removes more sputtered atoms from the surface of the cathode, increasing the density in the plasma. The atoms are carried onto the sampling aperture by the flow and it is not just left to the forces of diffusion. Third, the plasma gets chance to cool and the energy transfer to Cu becomes more probable either by interaction with  $\text{Ar}(4s, ^3P)$  or with higher-energy states. Of course, if the flow is too slow these advantages become offset by losses, such as radial diffusion and quenching or condensation at the walls, or indeed by collision.

### V. CONCLUSION

A fast-flow glow discharge ion source has been described, fitted to a high-resolution magnetic deflection mass spectrometer. Without a negative bias potential on the sampling cone aperture, the field and sheath potentials in the plasma opposed the transfer of cations through sampling aperture into the mass spectrometer. Nevertheless, copious ion currents were recorded at the fastest-flow speeds. It is inferred that these were created by field ionization of neutral excited states emanating from the plasma. This is supported by the relative lack of ionization for the same experiment conducted with a quadrupole analyzer, in which the ionizing or accelerating field is much lower, and by the differences in spectra generated. Further evidence comes from the behavior observed when a negative bias voltage is applied to the sample cone. Under the fastest-flow conditions, the detected ion signal decreases; this is opposite to the behavior expected if free ions are present in the plasma. However, it can be explained if the applied voltage destabilizes the excited states before they get through the sample aperture, removing them from the flux of field-ionizable atoms in the gas effusing from the source into the high field accelerating region of the mass spectrometer. Under slower flow rate conditions, the plasma species will be at a lower average energy. The Stark effect can then lift the excited state energy without releasing the electron. Such states then become more readily field ionizable when they leave the cell and the current goes up with the increasing cone voltage. There is an intermediate plasma state in which the low cone field causes the latter effect, but the higher cone bias causes the former and the curve goes through a maximum.

The excited states being detected must be high  $n$  and  $l$  Rydberg atoms and molecules, stabilized by the plasma environment. The reaction of very small quantities of  $\text{H}_2$  gas titrated into the plasma boundary region, removed most discharge gas ions from the spectrum, boosted the  $\text{Cu}^+$  signal, suppressed the conductivity of the electric current through the plasma, but did not cause significant changes to the field,

<sup>1</sup>Therefore not field ionizable.



sheath, and wall potentials. This ruled out the possibility of an ion-molecule reaction to form  $\text{ArH}^+$  followed by a rapid recombination with electrons in the plasma. The effect was the same, even when a negative extraction voltage was applied to the cone. These results indicated that free  $\text{Ar}^+$  ions and electrons were less important in this region of the plasma than the excited state processes and supports our previous interpretation [5]. The lifetimes of the detected Ar Rydberg atoms inside the flowing plasma are in the region of  $(1-10) \times 10^{-4}$  s. This is an order of magnitude longer than that measured under nonplasma low pressure conditions. It suggests that the plasma environment helps stabilize Rydberg species, which gives support to the idea that they may have a

much more significant role in the mechanism sustaining higher pressure plasmas than has hitherto been considered. This is in the process of further investigation.

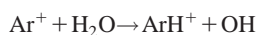
#### ACKNOWLEDGMENTS

We gratefully acknowledge help, with the cathode erosion measurements, of Claire Wills of the Chemistry Department and Des Thomas, John Tregembo, and Stuart Jones of the Chemistry Department technical services for their help in building the apparatus. We thank the EPSRC for a grant and a financial support (IPM), and (VG) Thermo Elemental for financial support.

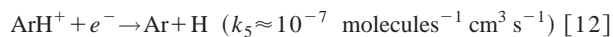
- 
- [1] B. Chapman, *Glow Discharge Processes* (Wiley, New York, 1980).
- [2] F. Llewellyn-Jones, *The Glow Discharge and an Introduction to Plasma Physics* (Methuen, London, 1966).
- [3] A recent paper studying this effect is by A. Belkind and F. Jansen, *Surf. Coat. Technol.* **99**, 52 (1998).
- [4] L. B. Loeb, *Fundamental Processes of Electrical Discharge in Gases* (Wiley, New York, 1939).
- [5] R. S. Mason, P. D. Miller, and I. P. Mortimer, *Phys. Rev. E* **55**, 7462 (1997).
- [6] A. Bogaerts and R. Gijbels, *J. Anal. At. Spectrom.* **15**, 441 (2000).
- [7] H. W. Drawin, in *Plasma Diagnostics*, edited by W. Lochte-Holtgreven, American Vacuum Society Classics (AIP Press, New York, 1995), Chap. 13, p. 777.
- [8] J. W. Coburn and E. Kay, *Appl. Phys. Lett.* **19**, 350 (1971).
- [9] F. L. King and W. W. Harrison, *Mass Spectrom. Rev.* **9**, 285 (1990).
- [10] R. S. Mason, I. P. Mortimer, D. R. Williams, and D. Gilmour, in *Proceedings of the XIV International Conference on Gas Discharges and their Applications, 2002*, GD2002 Local Organizing Committee (University of Liverpool, Liverpool, 2002), Vol. 2, p. 252.
- [11] P. F. Knewstubb and A. W. Tickner, *J. Chem. Phys.* **36**, 684 (1962).
- [12] R. F. G. Meulenbroeks, A. J. Van Beek, A. J. G. Van Helvoort, M. C. M. Van Den Sanden, and D. C. Schram, *Phys. Rev. E* **49**, 4397 (1994); D. K. Otorbaev, A. J. M. Buuron, N. T. Guerassimov, M. C. M. Van Den Sanden, and D. C. Schram, *J. Appl. Phys.* **76**, 4499 (1994).
- [13] T. F. Gallagher, *Rydberg Atoms* (Cambridge University Press, Cambridge, 1994).
- [14] P. D. Miller, D. W. Thomas, R. S. Mason, and M. Leizers, in *Proceedings of the Fourth International Conference on Plasma Source Mass Spectrometry, Durham 1994*, edited by G. Holland (University of Durham, Durham, 1995).
- [15] D. J. Mitchell, N. A. Dash, and R. S. Mason, in *Proceedings of the XIV International Conference on Gas Discharges and their Applications, 2002*, GD2002 Local Organizing Committee (University of Liverpool, Liverpool, 2002), Vol. 2, p. 248.
- [16] R. S. Mason and D. M. P. Milton, *Int. J. Mass Spectrom. Ion Processes* **91**, 209 (1989).
- [17] 4 kV was the safe working voltage to avoid electrical breakdown of the plasma jet emanating from the ion exit.
- [18] D. J. Mitchell, Ph.D. thesis, University of Wales Swansea, 2002.
- [19] The value of the discharge current was sensitive to the size of the cathode used.
- [20] The voltage between two points was measured, with zero current flowing ( $< 2 \times 10^{-7}$  A) through the external circuit.
- [21] D. R. Williams, Ph.D. thesis, University of Wales Swansea, 2001.
- [22] R. S. Mason and M. Pichilingi, *J. Phys. D* **27**, 2363 (1994).
- [23] P. F. Knewstubb and A. W. Tickner, *J. Chem. Phys.* **36**, 674 (1962); W. Lindinger, *Phys. Rev. A* **7**, 328 (1973).
- [24] P. D. Miller, Ph.D. thesis, University of Wales Swansea, 1996.
- [25] H. J. Kim, E. H. Piepmier, G. L. Beck, G. G. Brumbaugh, and O. T. Farmer, III, *Anal. Chem.* **62**, 639 (1990); **62**, 1368 (1990).
- [26] I. P. Mortimer, Ph.D. thesis, University of Wales Swansea, 2000.
- [27] D. W. Setser, *Reactive Intermediates in the Gas Phase—Generation and Monitoring* (Academic Press, New York, 1979), Chap. 3, p. 151.
- [28] R. L. Smith, D. Serxner, and K. R. Hess, *Anal. Chem.* **61**, 1103 (1989).
- [29] W. Vieth and J. C. Huneke, *Spectrochim. Acta, Part B* **45**, 941 (1990).
- [30] E. B. M. Steers and F. Lies, *J. Anal. At. Spectrom.* **4**, 199 (1989); K. Wagatsuma and K. Hirokawa, *Spectrochim. Acta, Part B* **51**, 349 (1996); A. Bogaerts and R. Gijbels, *J. Anal. At. Spectrom.* **11**, 841 (1999).
- [31] A. Bogaerts and R. Gijbels, in *Glow Discharge Optical Emission Spectrometry*, edited by R. Payling, D. Jones, and A. Bengston (Wiley, New York, 1997), Chap. 4, p. 176.
- [32] J. A. Sciavone, S. M. Tarr, and R. S. Freund, *Phys. Rev. A* **20**, 71 (1979).
- [33] R. S. Mason, P. D. J. Anderson, and M. T. Fernandez, *Int. J. Mass Spectrom. Ion Processes* **128**, 99 (1993).
- [34] In Kim's and Pipmeier's quadrupole based experiments [25] a voltage between 40 and 50 V was required, the flow rates used being half that of our experiments, although the pressure was not specified.
- [35] Recent experiments at Swansea, although on a different appa-

ratus, showed that a negative cone bias up to 100 V did not penetrate as far as 3 mm into the flowing plasma; Karla Newman (unpublished).

- [36] L. Schott, in *Plasma Diagnostics*, edited by W. Lochte-Holtgreven, American Vacuum Society Classics (AIP Press, New York, 1995), Chap. 11, p. 705.
- [37] The mechanism should operate whether the field applied at the cone is positive or negative. Recent experiments, employing a positive cone bias, showed this to be the case [17].
- [38] I. Dotan and W. Lindinger, *J. Chem. Phys.* **76**, 4972 (1982).
- [39] E. W. McDaniel, *Collision Phenomena In Ionised Gases* (Wiley, New York, 1964).
- [40] For example,  $\text{ArH}^+$ , if formed by an ion-molecule reaction with water, would also be removed by recombination. At 2 Torr pressure in argon, the formation and removal processes are both much faster than radial diffusion to the walls and the steady state concentration of  $\text{ArH}^+$  would be dominated by the reactions:



$$(k' = 1.6 \times 10^{-9} \text{ molecules}^{-1} \text{ cm}^3 \text{ s}^{-1})$$



Under steady state conditions  $[\text{Ar}]/[\text{ArH}^+] = k_5[e^-]/k'[\text{H}_2\text{O}] \approx 100$ , assuming commercial argon gas typically contains <4 ppm of  $\text{H}_2\text{O}$ , pressure being 2 Torr at 320 K, and making very modest assumptions about the electron density in a conventional plasma [1] as  $10^{11} \text{ cm}^{-3}$  ( $<3 \times 10^{-4}\%$  ionization). Y. Ikezoe, S. Matsuoka, M. Takebe, and A. Viggiano, in *Proceedings of the International Conference on Gas Phase Ion-Molecule Rate Constants Through 1986* (Maruzen Company, Ltd., Tokyo, 1986).

- [41] V. D. Hodoroaba, V. Hoffman, E. B. M. Steers, and K. Wetzig, *J. Anal. At. Spectrom.* **15**, 951 (2000); **15**, 1075 (2000); **16**, 431 (2001).
- [42] F. Merkt, *J. Chem. Phys.* **100**, 2623 (1994).
- [43] J. A. Schiavone, D. E. Donohue, D. R. Herrick, and R. S. Freund, *Phys. Rev. A* **16**, 48 (1977).
- [44] R. S. Mason, P. D. J. Anderson, and M. T. Fernandez, *Int. J. Mass Spectrom. Ion Processes* **128**, 99 (1993).
- [45] F. Merkt and R. N. Zare, *J. Chem. Phys.* **101**, 3495 (1994).
- [46] In a different apparatus fitted with windows at the sample cone, a glow was observed along the flowing plasma, up to the cone.